Frontiers of Information Technology & Electronic Engineering
www.jzus.zju.edu.cn; engineering.cae.cn; www.springerlink.com
ISSN 2095-9184 (print); ISSN 2095-9230 (online)
E-mail: jzus@zju.edu.cn

Swarm intelligent computing of electric eel foraging heuristics for fractional Hammerstein autoregressive exogenous noise model identification#

Faisal ALTAF[1], Ching-Lung CHANG[2], Naveed Ishtiaq CHAUDHARY[†‡3], Taimoor Ali KHAN[4], Zeshan Aslam KHAN[4,5], Chi-Min SHU[6], Muhammad Asif Zahoor RAJA[3]

[1]*Editorial Graduate School of Engineering Science and Technology, National Yunlin University of Science and Technology, Yunlin 64002, Taiwan, China*

[2]*Department of Computer Science and Information Engineering, National Yunlin University of Science and Technology, Yunlin 64002, Taiwan, China*

[3]*Future Technology Research Center, National Yunlin University of Science and Technology, Yunlin 64002, Taiwan, China*

[4]*International Graduate School of Artificial Intelligence, National Yunlin University of Science and Technology, Yunlin 64002, Taiwan, China*

[5]*Department of Electrical and Computer Engineering, International Islamic University, Islamabad 44000, Pakistan*

[6]*Department of Safety, Health and Environmental Engineering, National Yunlin University of Science and Technology, Yunlin 64002, Taiwan, China*

[†]E-mail: chaudni@yuntech.edu.tw

Received Aug. 20, 2024; Revision accepted Dec. 1, 2024; Crosschecked

Abstract: The knacks of fractional calculus are considered a useful tool to obtain a deeper insight into systems considering the memory effect or previous history. Fractional order modeling of nonlinear systems may increase the stiffness and complexity of the system but also provides better insights. This study introduces swarm intelligence-based parameter estimation of the fractional Hammerstein autoregressive exogenous noise (fractional-HARX) model. The Grunwald–Letnikov finite difference formula is used to develop the fractional-HARX model from the standard Hammerstein autoregressive exogenous noise model. This study presents the design of a swarm intelligence-based electric eel foraging optimization algorithm (EEFOA) for parameter estimation of the fractional-HARX model under multiple noise scenarios for 2nd and 3rd-order polynomial type nonlinearity. The key term separation principle is also incorporated in the system model to reduce the occurrence of redundant parameters due to cross-product terms in the information vector. The designed methodology is examined, and the superiority of EEFOA is endorsed in terms of convergence, robustness, stiff parameter estimation, and deviation from the mean point in comparison with state-of the-art optimization heuristics such as the whale optimization algorithm, the African vulture optimization algorithm, Harris hawk's optimizer, and the reptile search algorithm. The statistical significance of the EEFOA for the estimation of fractional-HARX models is also established using statistical indices of best, mean, and worst fitness values along with standard deviation for multiple noise scenarios.

Key words: Fractional calculus; Nonlinear systems; Electric eel foraging; Intelligent computing
https://doi.org/10.1631/FITEE.2400730 **CLC number:**

1 Introduction

Fractional calculus has been utilized to simulate several mathematical and physical processes in a diverse variety of domains (Megherbi et al., 2024; Sweis et al., 2023; Frikh et al., 2024), including dig-

‡ Corresponding author

Electronic supplementary materials: The online version of this article (https://doi.org/10.1631/FITEE.2400730) contains supplementary materials, which are available to authorized users

ital image processing (Gamini et al., 2023), engineering (Partohaghighi et al., 2024), biomedicine (Ionescu et., 2017; Mukhtar et al., 2024), control systems (Li Z et al., 2023a; Zhang X, et al., 2023), power systems (Sowa et al., 2023, Padhi et al., 2023), signal processing (Machado et al., 2015; Karaca et al., 2023), electrical circuits (Kausar et al., 2024), and stress detection (Šapina et al., 2020). Additionally, its applications include lithium–ion batteries (Wang S et al., 2024), fractional neural networks (Li S et al., 2023), and the modeling of COVID-19 transmission (Mehmood N et al., 2023), hybrid viscous nanofluids (Ali et al., 2021), and nuclear reactors (Vyawahare et al., 2013). The advantageous knacks of fractional calculus are beneficial for enhanced mathematical modeling and gaining better insights of systems. The Hammerstein model, which includes the combination of nonlinear static and dynamic linear blocks, is used in the modeling of various nonlinear systems (Zhang F et al., 2024; Zhang MG et al., 2024; Li F et al., 2023a; Li F et al., 2023b). The structure allows simplified and powerful representation of complex systems, making it a valuable tool for real-world applications. The identification of the Hammerstein nonlinear system is considered a challenging task due to its stiffness and complexity (Hu et al., 2024; Li F et al., 2024; Liu et al., 2023; Li F et al., 2023c). The employment of fractional calculus is also involved in Hammerstein or input nonlinear systems for improved insight into the complex system (Altaf et al., 2024; Khan et al., 2024a; Khan et al., 2024b; Malik MF et al., 2023).

Metaheuristics have proven to be highly efficient in solving complex problems in diversified fields (Ye et al., 2023), for instance, identifying electro-hydraulic actuator systems (Mehmood K et al., 2024), biomedical engineering (Han et al., 2023), feature selection (Fang et al., 2023), microelectronics and nanophotonics (Jakšić et al., 2023). In addition, applications of the swarm intelligence-based algorithms can be found in hydraulic performance prediction (Rahmanshahi et al., 2024), supply chain management (Ala et al., 2024), estimation of multi-frequency sinusoidal signaling (Malik NA et al., 2024), big data predictive modeling (El-Hasnony et al., 2020), data mining (Baburaj 2022), spam detection (Tubishat et al., 2023), economic emission dispatching (Dong et al., 2023), machine learning (Abdollahzadeh et al., 2024), and cancer diagnosis (González et al., 2019). These investigations serve as the driving forces for authors to delve into the newly proposed bio-inspired algorithm known as the electric eel foraging optimization algorithm (EEFOA). EEFOA was proposed by Weiguo Zhao et al. in 2024 (Zhao et al., 2024). EEFOA is influenced by the sophisticated collective foraging activities displayed by electric eels in their natural habitat. The mathematical model is based on searching behavior, including migration, hunting, resting, and interaction. The proposed optimization technique allows exploration and exploitation at the same stage of optimization. Moreover, the energy factor is devised to regulate the shift from global search to local search while maintaining an optimal balance. The efficacy of EEFOA is validated by making a comparison with 12 other algorithms out of 23 test functions with CEC 2011 and CEC 2017 test packages. The test results demonstrate the overwhelmingly superior performance of EEFOA in comparison with other algorithms. The effectiveness of EEFOA is thoroughly evaluated through the examination of 10 engineering challenges, including sluice opening control management in a hydro-power facility under disaster tripping situations.

The results indicate the superior performance and great potential of EEFOA in addressing various complex real-world challenges. The knacks of EEFOA in solving complex problems and real-world challenges motivated the authors to exploit EEFOA for a given problem. The primary objective of this research is to investigate the use of bio-inspired EEFOA for stiff parameter estimation of the fractional-HARX model with key term separation for multiple polynomial type nonlinearities and noise variations in comparison with the state-of-the-art of optimization heuristics such as the whale optimization algorithm (Mirjalili et al., 2016), the African vulture optimization algorithm (Abdollahzadeh et al., 2021), Harris hawk's optimizer (Heidari et al., 2019), and the reptile search algorithm (Abualigah et al., 2022). The key term separation principle is incorporated to reduce the occurrence of redundant parameters due to cross-product terms in the information vector of the system (Wang D, 2024). The innovative contributions of the scheme are succinctly outlined as follows:

- The swam intelligent computing of EEFOA is

efficaciously exploited to estimate the parameters of a fractional Hammerstein autoregressive system with exogenous noise.

- The key term separation principle is incorporated to reduce the complexity by avoiding the redundant parameters that occur due to cross-product terms in the information vector.
- The value of the devised optimization technique is confirmed by way of experimentation in several noisy environments considered in the fractional-HARX model with multiple orders of nonlinearity.
- The efficacy of the proposed EEFOA is endorsed through its robust, accurate, convergent, and stable performance in comparison with state-of-the-art optimization heuristics.

The remainder of the paper is organized as follows: Section 2 introduces the fractional-HARX model and the system model based on fractional calculus. Section 3 comprehensively explains the proposed methodology for estimating the parameters of the fractional-HARX model. This includes the formulation of the objective function, EEFOA, and a description of the performance metric. Section 4 presents the results of the methodology and provides a detailed interpretation of the findings. Section 5 provides the concluding thoughts and comments on potential areas for future investigation.

2 Fractional HARX Model

The fractional-HARX model is represented by a block structure diagram in Fig.1. where $m(t)$ represents input, $c(t)$ presents output, and exogenous noise is represented by $u(t)$, as mathematically expressed in Equation (1):

$$c(t)=\frac{J(z)}{K(z)}\bar{m}(t)+\frac{1}{K(z)}u(t), \tag{1}$$

where the polynomials $K(z)$ and $J(z)$ having fractional order γ are given as:

$$K(z)=1+k_1(z^{-1})^{\gamma}+k_2(z^{-2})^{\gamma}+...+k_{n_k}(z^{-n_k})^{\gamma}, \tag{2}$$

$$J(z)=j_0+j_1(z^{-1})^{\gamma}+j_2(z^{-2})^{\gamma}+...+j_{n_j}(z^{-n_j})^{\gamma}. \tag{3}$$

The output of the nonlinear block in the model is obtained by applying nonlinear function f, as expressed below:

$$\bar{m}(t)=f(m(t)), \tag{4}$$

$$f(m(t))=[f_1(m(t)),\ f_2(m(t)),...,\ f_{l_r}(m(t))], \tag{5}$$

$$\begin{aligned}\bar{m}(t)&=r_1m(t)+r_2(m(t))^2+...+r_{n_r}(m(t))^{n_r}\\&=\sum_{j=1}^{n_r}r_j f_j(m(t))\end{aligned} \tag{6}$$

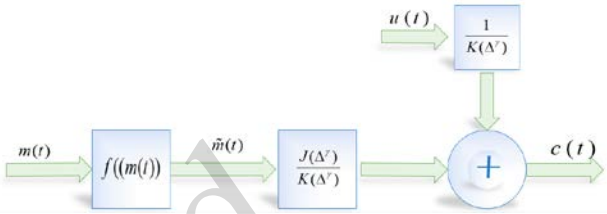

Fig.1 Fractional-HARX block diagram

The significance of fractional order derivatives is to be used for solving the differentiation into non integer order. Multiple mathematical operators defining fractional order derivatives have been introduced by the research community, such as the Atangana–Baleanu and Caputo–Fabrizio derivatives. (Riemann–Liouville and Caputo exist with varying properties and interpretations)**,** the Hilfer fractional derivative, the Liouville–Caputo derivative, the Katugampola fractional derivative, and the Grünwald–Letnikov fractional derivative (GL-FD). The GL-finite difference operator for $c(t)$ where $t=ab$ — where *a* is the sampling size and the total number of samples are given as *b*—the expression is formulated as (Malik MF et al., 2022):

$$\begin{aligned}&D^{\gamma}[c(ab)]=\frac{1}{b^{\gamma}}\sum_{i=0}^{\lceil\gamma\rceil}(-1)^i\binom{\gamma}{i}c(a-ib),\\&\binom{\gamma}{i}=\begin{cases}1 & i=0\\ \dfrac{\gamma(\gamma-1)...(\gamma-i+1)}{i!} & i>0\end{cases}.\end{aligned} \tag{7}$$

Now, by putting Equations (2), (3), and (6) into Equation (1):

$$c(t)=-\sum_{i=1}^{n_k}k_iD^{\gamma}[c(t-i)]+\sum_{i=0}^{n_j}j_iD^{\gamma}[\bar{m}(t-i)]+u(t). \tag{8}$$

The key term separation technique is a valuable tool used in system identification, particularly for non-

linear systems like the Hammerstein model. It helps to achieve better parameter estimation by avoiding the estimation of redundant parameters, ultimately leading to a more efficient identification process. Consider $\bar{m}$ a key term and assume $j_0 = 1$

$$c(t) = -\sum_{i=1}^{n_k} k_i D^\gamma [c(t-i)] + j_0 D^\gamma [\bar{m}(t)] + \sum_{i=1}^{n_j} j_i D^\gamma [\bar{m}(t-i)] + u(t), \quad (9)$$

$$c(t) = -\sum_{i=1}^{n_k} k_i D^\gamma [c(t-i)] + \sum_{i=1}^{n_j} j_i D^\gamma [\bar{m}(t-i)] + D^\gamma \sum_{i=1}^{n_p} r_i f_i(m(t)) + u(t). \quad (10)$$

The parameter and corresponding information vectors are expressed as:

$$\boldsymbol{\omega}_k(t) = [-D^\gamma c(t-1), -D^\gamma c(t-2), ..., -D^\gamma c(t-2), ..., -D^\gamma c(t-n_k)]^T, \quad (11)$$

$$\boldsymbol{\omega}_j(t) = [\bar{m}(t-1), \bar{m}(t-2), ..., \bar{m}(t-m_j)]^T, \quad (12)$$

$$\boldsymbol{\omega}_r(t) = [\, f_1[m(t)],\, f_2[m(t)], ..., \, f_{n_r}[m(t)]]^T. \quad (13)$$

$$\mathbf{k} = \left[k_1, k_2, \ldots, k_{n_k} \right]^T, \quad (14)$$

$$\mathbf{j} = \left[j_1, j_2, \ldots, j_{n_j} \right]^T, \quad (15)$$

$$\mathbf{r} = \left[r_1, r_2, \ldots, r_{n_r} \right]^T. \quad (16)$$

At this stage, the key term-separated fractional-HARX model is given as:

$$c(t) = \boldsymbol{\omega}_k^T(t)\mathbf{k} + \boldsymbol{\omega}_j^T(t)\mathbf{j} + \boldsymbol{\omega}_r^T(t)\mathbf{r} + u(t). \quad (17)$$

The corresponding fitness function for the fractional-HARX model in terms of mean square error sense via the difference between $c(t)$ (actual response) and $\hat{c}(t)$ (estimated response) is formulated as;

$$Fitness = mean\left[\left(c(t) - \hat{c}(t) \right)^2 \right]. \quad (18)$$

The estimated response of the fractional HARX model is given as:

$$\hat{c}(t) = \boldsymbol{\omega}_k^T(t)\hat{\mathbf{k}} + \boldsymbol{\omega}_j^T(t)\hat{\mathbf{j}} + \boldsymbol{\omega}_r^T(t)\hat{\mathbf{r}}, \quad (19)$$

and the unknown parameter vector is given as:

$$\hat{\mathbf{k}} = \left[\hat{k}_1, \hat{k}_2, \ldots, \hat{k}_{n_k} \right]^T, \quad (20)$$

$$\hat{\mathbf{j}} = \left[\hat{j}_1, \hat{j}_2, \ldots, \hat{j}_{n_j} \right]^T, \quad (21)$$

$$\hat{\mathbf{r}} = \left[\hat{r}_1, \hat{r}_2, \ldots, \hat{r}_{n_r} \right]^T. \quad (22)$$

3 Methodology

The EEFOA is a fascinating newly developed bio-inspired optimization algorithm proposed in 2024 based on the collective search behavior of electric eels in their environment. The EEFOA mimics the important four key foraging behaviors of electric eels, i.e., interaction, resting, hunting, and migration.

These four important behaviors are mathematically modelled for crucial aspects of electric eels. The transition between exploration and exploitation is dynamically controlled by an "energy factor" depending on search progress. However, it is most essential to ensure the adaptability to different problem landscapes. The EEFOA flow chart is provided in Fig. 2.

3.1. Interaction Phase

A solution vector containing the optimizing variables is represented by an eel in the population. The fitness is computed on the basis of the objective function of the specific problem. In the interaction phase, eels collaborate to explore the search space.

Eels transmit electric pulses and receive signals from other eels. This is known as electrolocation and is represented by a function in which the orientation (distance and direction) of neighboring eels is calculated. However, based on a probability-based function depending upon fitness and distance, the eels share the best position found. Each individual eel's position is updated depending on its own position established by the information of neighbors and the random term for exploration.

An electric eel within the environment can interact randomly with any other eels within the population by using the regional information (the search space). A churn is a random movement in various directions, and is marked by the interaction of an eel. Mathematically, the churn is modelled as:

$$Q = n_1 \times W \tag{23}$$

$$n_1 \sim N(0,1) \tag{24}$$

$$W = [w_1, w_2, ...w_k, ..., w_d] \tag{25}$$

$$w(\mathrm{k}) = \begin{cases} 1\,if & k == s\{m \\ 0 & else \end{cases} \tag{26}$$

$$s = randperm(d) \tag{27}$$

$$m = 1, ..., \left\lceil \left(\frac{L-l}{l} \times r_1 \times (\mathrm{d}-2) + 2 \right) \right\rceil, \tag{28}$$

where L = maximum iterations. Hence, interacting behavior is given as:

$$\begin{aligned} &If\ \ fitness(y_j(t)) < fitness(y_i(t)) \\ &\begin{cases} s_i(t+1) = y_j(t) + Q \times (\bar{y}(t) - y_i(t)) c_1 > 0.5 \\ s_i(t+1) = y_j(t) + Q \times (y_r(t) - y_i(t)) c_1 \le 0.5 \end{cases} \\ &If\ \ fitness(y_j(t)) \ge fitness(y_i(t)) \\ &\begin{cases} s_i(t+1) = y_i(t) + Q \times (\bar{y}(t) - y_j(t)) c_2 > 0.5 \\ s_i(t+1) = y_i(t) + Q \times (y_r(t) - y_j(t)) c_2 \le 0.5 \end{cases} \end{aligned} \tag{29}$$

$$y(t) = \frac{1}{n} \sum_{i=1}^{n} y_i(t) \tag{30}$$

$$y = Low + r \times (Up - Low), \tag{31}$$

where the variable represents:

c_1 and c_2 : random numbers between (0,1), $fitness(y_i(t))$: the fitness of the i^{th} electric eel candidate position, y_j : the randomly selected eel position, $r_{1:}$ a random number within (0,1).

3.2. Resting Phase

This phase mimics eels potentially updating their respective positions and taking breaks. During this phase, the rest probability of an eel entering this phase is determined by a random number generator. However, during this phase the eels exploit the neighborhood in their respective search space.

The mathematical expression to define the rest area is given as:

$$\left\{ X \,|\, X - V(t) \right| \le \mu_0 \times \left| V(t) - y_{prey}(t) \right| \right\} \tag{32}$$

$$\mu_0 = 2 \cdot \left(\varepsilon - \varepsilon^{\frac{1}{L}} \right) \tag{33}$$

$$V(t) = Low + v(t) \times (Up - Low) \tag{34}$$

$$v \begin{cases} l = \dfrac{y_{rand\{n}^{rand\{d} \{ l - Low^{rand\{d}}{Up^{rand\{d} - Low^{rand\{d}}. \end{cases} \tag{35}$$

The variables are defined as:

y_{prey} is the position vector, μ_0 is the resting area initial value, $\mu_0 \times \left| V(t) - y_{prey}(t) \right|$ is the resting area range. $y_{rand\{n}^{rand\{d}$ represents the random position of a randomly selected individual and V represents a normalized number.

$$R_i(t+1) = V(t) + \mu \times \left| V(t) - y_{prey}(t) \right| \tag{36}$$

$$\mu = \mu_0 \times \sin(2\Pi r_2). \tag{37}$$

μ is the resting area scale and r_2 is the random number (0,1).

As the iteration proceeds, the resting area range decreases, enhancing the exploitation. As the resting area is determined, the eels move towards it by updating their position towards the resting area. This behavior can be mathematically expressed as:

$$\begin{aligned} s_i(t+1) &= R_i(t+1) \\ &+ n_2 \times (R_i(t+1) round(rand) \times y_i(t)) \end{aligned} \tag{38}$$

$$n_2 \sim N(0,1). \tag{39}$$

3.3. Hunting Phase

Instead of directly hunting the prey selected in the search space, the eels make a large circle around the prey and start peer to peer communication by transmitting low voltage signals. As the eels' communication increases, the circle shrinks and the eels drive the prey towards the shallow end. However, after being frightened, the prey move into the electrically charged circle and update their respective

positions, that is, their position with respect to their current position in the hunting space. Mathematically, the hunting area is expressed as:

$$\left\{X \left| X - y_{prey}(t) \right| \le \eta_0 \times \left| \overline{y}(t) - y_{prey}(t) \right| \right\} \quad (40)$$

$$\eta_0 = 2 \cdot \left(\varepsilon - \varepsilon^{\frac{1}{L}} \right), \quad (41)$$

where η_0 is the hunting area scale, y_{prey} is the eel centering on the prey.

The updated position of the prey with respect to their previous position in the hunting area is expressed as:

$$H_{prey}(t+1) = y_{prey}(t) + \eta \times \left| \overline{y}(t) - y_{prey}(t) \right| \quad (42)$$

$$\eta = \eta_0 \times \sin(2\Pi r_3), \quad (43)$$

where η is the scale of the hunting area and r_3 is the random number (0,1). The mathematical notation of curling behavior is given as:

$$\begin{aligned} s_i(t+1) &= H_{prey}(t+1) \\ &+ \varpi \times (H_{prey}(t+1) - round(rand) \times y_i(t)) \end{aligned}, \quad (44)$$

where ϖ is the curling factor and is defined as:

$$\varpi = \varepsilon^{\frac{r_4(1-l)}{L}} \times \cos(2\Pi r_4), \quad (45)$$

where r_4 is random number (0,1).

3.4. Migrating Phase

The eel migrates from the resting phase to the migrating phase when it finds prey. Mathematically, this is expressed as:

$$\begin{aligned} s_i(t+1) = r_5 \times R_i(t+1) + r_6 \times A_r(t+1) \\ - D \times (A_r(t+1) - y_i(t)) \end{aligned} \quad (46)$$

$$A_r(t+1) = y_{prey}(t) + \eta \times \left| \overline{y}(t) - y_{prey}(t) \right|, \quad (47)$$

where A_r is a random position in hunting area, r_5 & r_6 are random numbers (0,1). $(A_r(t+1) - y_i(t))$ indicates the movement of prey towards the hunting area. D is the Lévy flight function, introduced for the exploitation phase of EFFOA to avoid becoming stuck in local minima.

To obtain the Lévy flight:

$$D = 0.001 \times \left| \frac{\nu - \theta}{|\vartheta|^{\frac{1}{x}}} \right| \quad (48)$$

$$\nu, \vartheta \sim N(0,1) \quad (49)$$

$$\theta = \left(\frac{\Gamma(1+x) \times \sin\left(\frac{\pi x}{2}\right)}{\Gamma\left(\frac{1+x}{2}\right) \times x \times 2^{\frac{x-1}{2}}} \right)^{\frac{1}{x}}, \quad (50)$$

where Γ is the gamma function and x=1.5

An eel observes the current position of the prey by transmitting an electric signal of low electric discharge and continuously observing the prey. If the foraging process is observed, the eel moves to the candidate position or otherwise stays in position. The position of the eels is updated by:

$$y_i(t+1) = \begin{cases} y_i(t) & fitness(y_i(t)) \le fitness(s_i(t+1)) \\ s_i(t+1) & fitness(y_i(t)) > fitness(s_i(t+1)) \end{cases}. \quad (51)$$

3.5. Energy Factor

An energy factor dynamically controls the shift between the exploration and exploitation phases. It decreases over time, increasing the focus on exploitation as the search progresses. Mathematically, the energy factor is computed as:

$$K(t) = 4 \times \sin\left(1 - \frac{l}{L}\right) \times \ln\frac{1}{r_7}. \quad (52)$$

r_7 is random number (0,1). From Equation (52), it can be seen that energy factor K decreases with increasing iterations. If K>1, the global search is completed, resulting in exploration. However, when the energy factor K≤1, local search is performed, resulting in exploitation.

For instance, the search mechanism of EEFOA with energy factor probability equals 1. The computational process is expressed as:

$$\sigma_K = 1 - \frac{l}{L}, \quad (53)$$

while the energy factor K is given by

$$K(t) = \sin(\sigma_K) \ln\frac{1}{r_7}. \quad (54)$$

The K's probability can be given as:

$$P\{K(t)>1\}=\frac{\int_0^1\int_0^{e^{-\frac{1}{4\sin(\sigma)}}}drd\sigma_K}{1}=-\int^{-\frac{1}{4\sin(1)}}-\alpha\frac{e^y dy}{y\sqrt{16y^2-1}}\approx 0.5035 \quad (55)$$

According to the expression in Equation (55), there is a 50% probability of execution in between exploration or exploitation while performing optimization.

3.6. Pseudo code

The pseudo code of EEFOA is presented in Algorithm 1, while the graphical abstract summarizes the suggested study according to the system model, the proposed plan, and the achieved results presented in Fig. 3.

Algorithm 1: Electric eel foraging optimization algorithm

Inputs: Features of best solution

Step 1. Set Parameters of EEFOA:
Number individual electric eels: n
Dimensions: d
Number of iterations: L
Execution of EEFOA
Step 2. Initialization
Initialize the random population: Y_i(i=1,2, 3,…,*n*)
Estimate fitness $Fitness_i$, and Y_{prey}
While,
the stopping criteria not met
do
Step 3. Calculate Energy Factor
For
Each individual eel Y_i
do
Calculate Energy Factor: K Using Eq. (42)
If (K>1)
Step 4. Interacting Phase
Interacting Phase: *w(k)* will take place using Eq. (29)
Evaluate $Fitness_i$
Else
Step 5. Resting Phase
If (Rand>1/3)
Determine the resting phase using Eq. (36)
Eel to execute resting-behavior using Eq. (38)
Calculate $Fitness_i$
***Else If (*Rand>2/3)**
Step 6. Migrating Phase
Execute migrating phase using Eq. (46)
Else
Step 7. Hunting
Calculate the hunting-region using Eq. (42)
Perform hunting using Eq. (44)
End If
End If
Update individual eel's position using Eq. (51)

End For
Update best solution Y_{prey}
End While
Return Y_{prey}
End

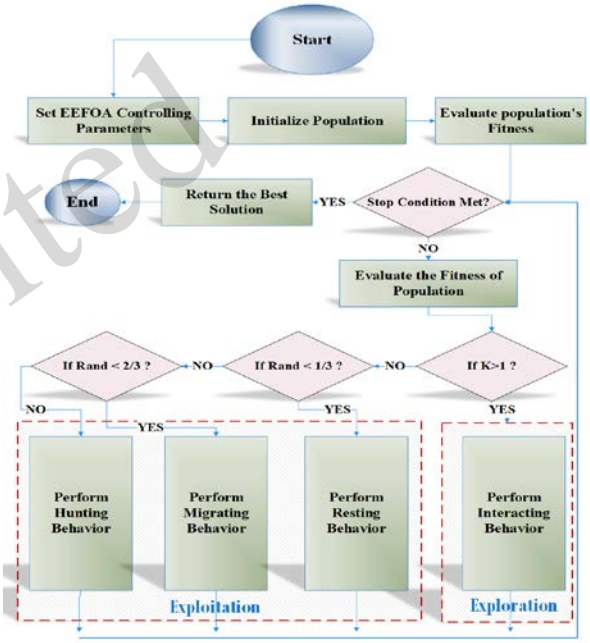

Fig. 2. Flow chart of EEFOA

4 Findings and Analysis

The outcomes of the computer-based simulation experiments are discussed in this section. The input signal is a random signal with zero mean and unit variance, while the Gaussian distributed signal with zero mean and constant variance is considered to be noise. The findings include the results and corresponding analysis after extensive simulations to elaborate the effectiveness of the recently proposed EEFOA for a fractional-HARX system. This section is divided into two sections: a fractional-HARX system with 2nd order nonlinearity and a fractional-HARX system with 4nd order nonlinearity. The

simulations are executed on Intel(R) Core (TM) i7-9700 CPU @ 3.00GHz 3.00 GHz with 40 GB DDR4 RAM.

4.1 Case study 1: Fractional H-CAR system with 2nd order nonlinearity

In this case study, knacks of EEFOA are exploited for a fractional-HARX system with an order of nonlinearity equal to 2. The system is represented by six parameters, i.e., $[k_1, k_2, j_1, j_2, r_1, r_2]$, where the fractional order is 0.4. The performance is accessed through five different noise scenarios, i.e., u = 0, u = 0.00015, u = 0.0015, u = 0.015, u = 0.15 , and a multiple evaluation metric. The tuned parameters of the proposed EEFOA are taken from Zhao W et al. (2024). The second order nonlinear fractional-HARX system is expressed as follows:

$$K(z) = 1 + 0.45(z^{-1})^{0.4} + 0.3(z^{-2})^{0.4} \quad (56)$$

$$J(z) = 0.16(z^{-1})^{0.4} + 0.56(z^{-1})^{0.4} \quad (57)$$

$$\bar{m}(t) = 0.35m(t) + 0.8m(t)^2, \quad (58)$$

where the parameter vector is given as:

$$\omega = [\omega_1, \omega_2, \omega_3, \omega_4, \omega_5, \omega_6]$$

$$\omega = [k_1, k_2, j_1, j_2, r_1, r_2] = [0.45, 0.29, 0.16, 0.56, 0.35, 0.8].$$

Initially the performance of the proposed EEFOA for fractional-HARX is assessed using convergence characteristics. The simulations are executed for five noise scenarios and 2000 iterations and 500 iterations for u = 0, u = 0.00015, u = 0.0015, u = 0.015, and u = 0.15, respectively. In order to analyze the convergence behavior and steady-state response efficiently, different numbers of iterations are selected. The system is also analyzed with 50, 100, and 150 search agents, but no significant change is observed. This is why 50 search agents are selected for the rest of the study.

Figure 4 presents the convergence plots of the best run over 60 independent runs for all noise scenarios. For u = 0.0, EEFOA achieves a commendable fitness value higher than [e-30]. While u = 0.00015, u = 0.0015, u = 0.015, and u = 0.15 have fitness values of [1.27892E-08], 1.42604E-06, 1.63598E-04, and 2.06484E-02, correspondingly. While EEFOA does a commendable job with the fractional-HARX system, its performance is negatively affected by increased noise. In addition, Table 1 also displays the statistics for the highest, average, and worst fitness levels, along with the matching fitness. Further, the efficacy of EEFOA is evaluated via statistical analysis.

The simulations are performed for 60 autonomous runs to examine the proof of convergence of EEFOA for fractional-HARX. For u = 0.00015, u = 0.0015, u = 0.015, and u = 0.15 , plots are given for 100, 200, 300, and 500 iterations. For instance, for u = 0.00015, it is observed that increasing the iteration count stabilizes the performance of EEFOA. All noise scenarios at 500 iterations provide consistent and stable fitness, as witnessed in Figure 5. However, EEFOA becomes consistent before 500 iterations. Generally, the statistical analysis indicates that EEFOA is very consistent, stable, and robust, as it provides consistent fitness in early iterations.

EEFOA's performance is also examined in terms of its exactness and correctness in the estimation of the desired parameters of the system. The weight estimation plot for all noise levels on the best independent run is presented in Figure (6-10). Experimentation demonstrates that increasing the noise level decreases the exactness in estimating the desired weights, as given in Table 1. For instance, for the no-noise scenario, the desired parameters are estimated exactly before 500 iterations. This depicts the EEFOA's speed in parameter estimation and approaching a steady state. Similarly, when we increase noise up to u = 0.015, the EEFOA still provides an accurate estimation of parameters to a very close value. In a very high noise scenario at level u = 0.15, the accuracy is slightly disturbed, as observed in Figure 10. Additionally, some fluctuations in the convergence curves are seen during the initial iterations and then become stable during the steady state. The results confirm the robustness of the EEFOA in estimating the parameters of a fractional-HARX system for different noise scenarios.

To delve deeper into the performance, bar charts presenting average accuracy are given in Figure 11. It is observed from both Figure 11 and Table 2 that the best fitness is very close to the average fitness, which indicates that the EEFOA's performance is very consistent and stable. On occasion, the best, average, and worst fitnesses are [1.42604E-06], [1.42606E-06], and [1.42668E-06] for $u = 0.00015$. The values are very close, indicating the competence of EEFOA in providing stable fitness over independent runs.

The further examination is based on Nash–Sutcliffe efficiency (NSE); the value of NSE ranges from -∞ to 1. A higher NSE value indicates a better performance of the model, and 1 indicates the best fit. Figure 12 presents the NSE-based learning curves for all noise levels. The investigation yields that the EEFOA achieves NSE values of [1], [0.999999], [0.99985],

and [0.993212] for noise levels of u = 0.0, u = 0.00015, u = 0.0015, and u = 0.015. These NSE values indicate the good performance of EEFOA in the identification of desired parameters. Moreover, for a very high noise level of u = 0.15, the NSE value achieved approaches zero, exhibiting the natural behavior of the system. However, the noise u = 0.015 is also high, but the EEFOA performs well up to that level of noise

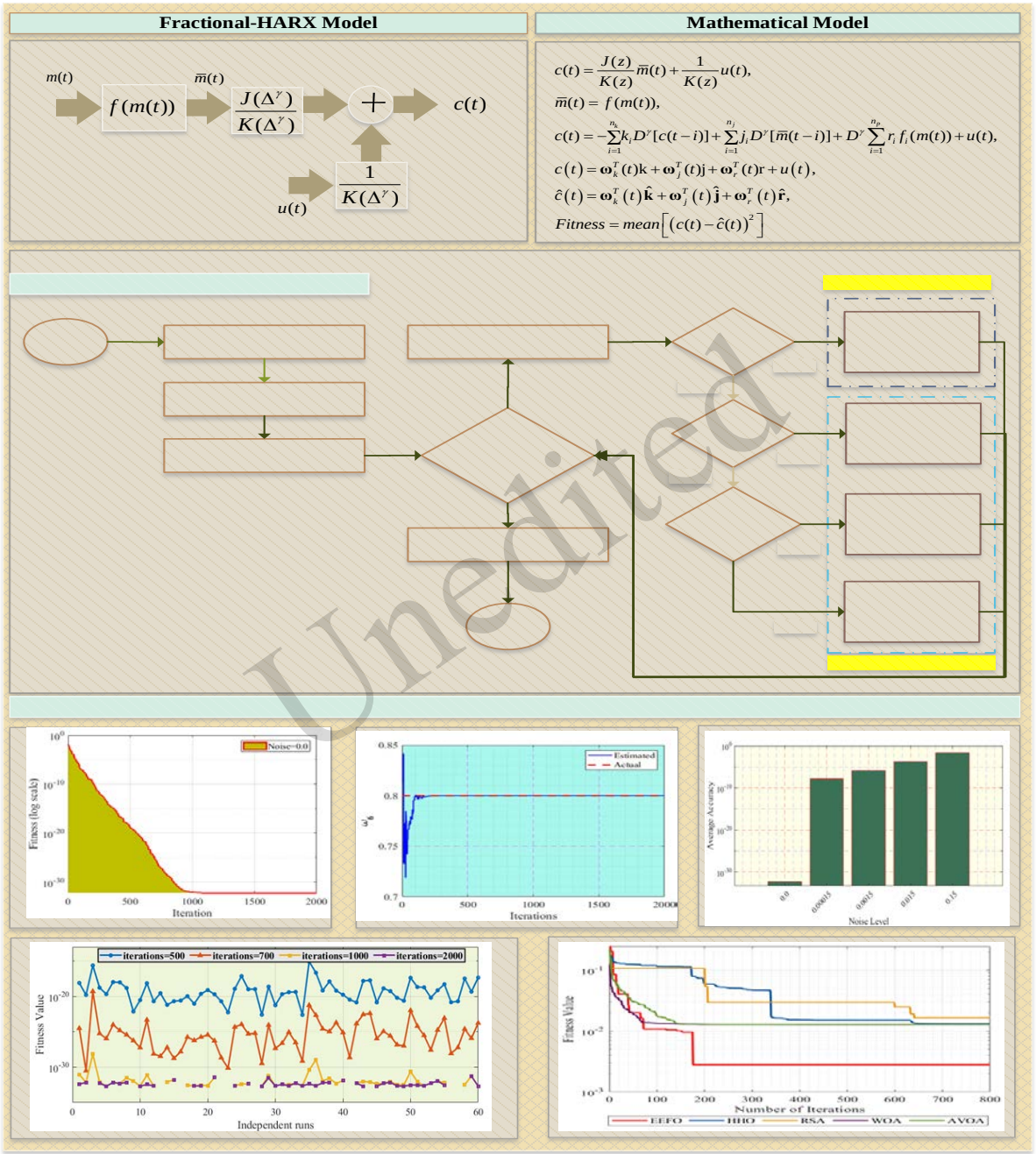

Fig. 3. Graphical abstract of the study

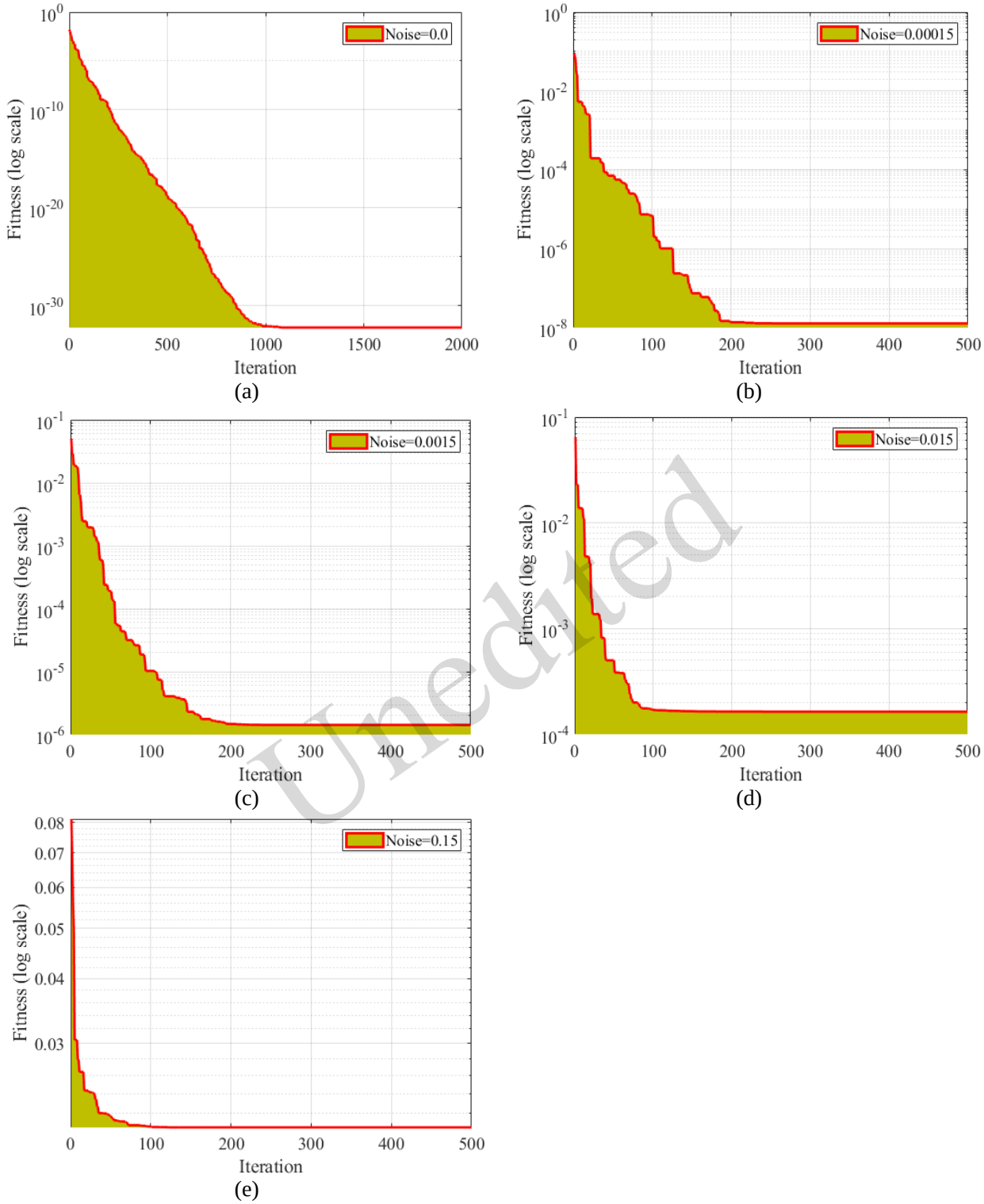

Fig. 4. Learning curves for all noise scenarios of case study 1

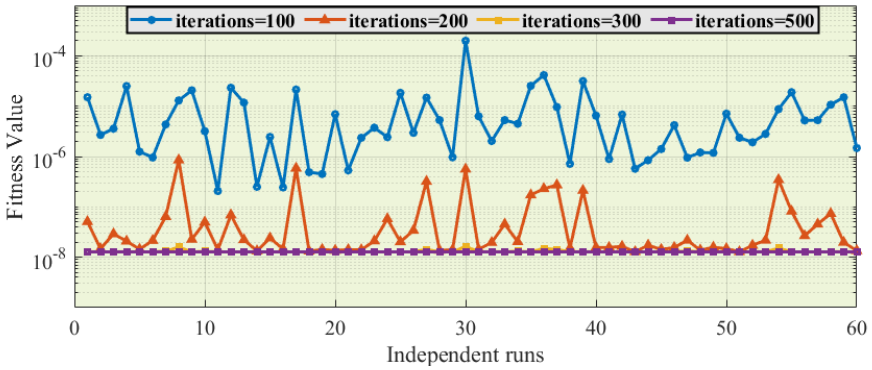

(a) $u = 0.00015$

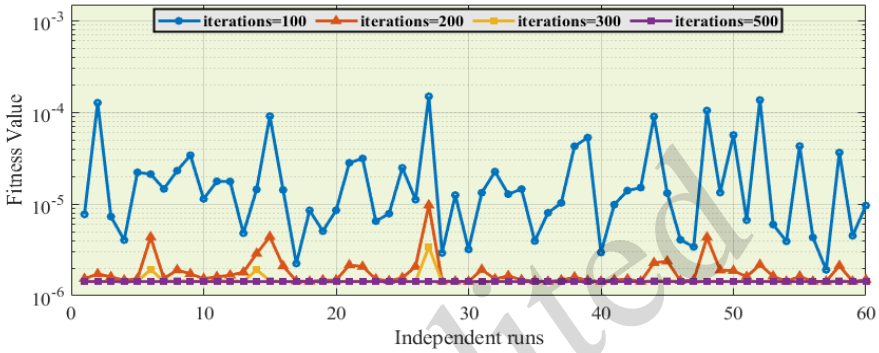

(b) $u = 0.0015$

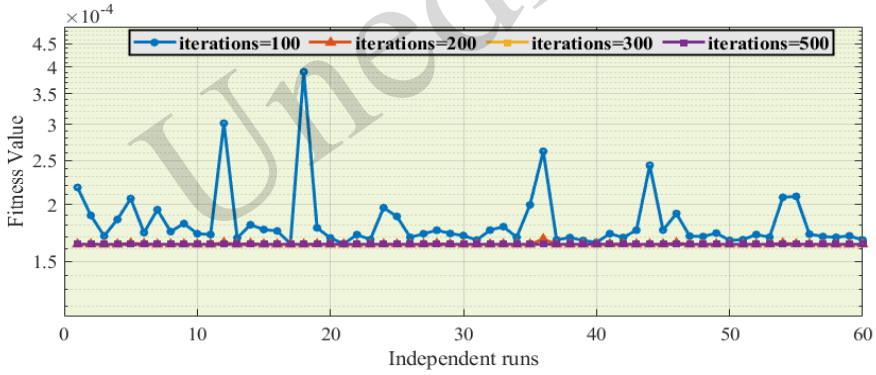

(c) $u = 0.015$

(d) $u = 0.15$

Fig. 5. Statistical plots at different iteration levels of case study 1

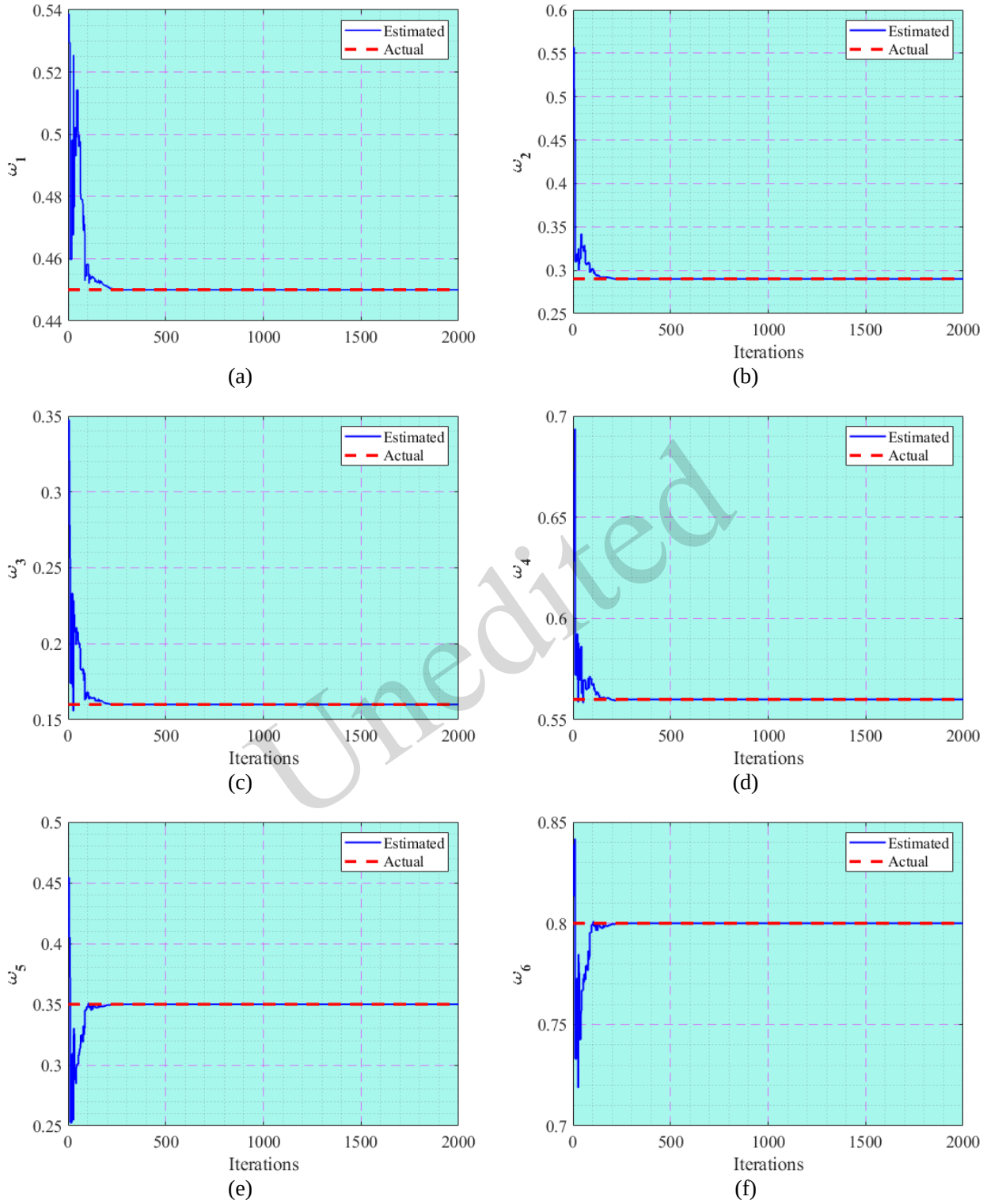

Fig. 6. Estimated parameters curves of the best independent run for $u = 0.0$ in case study 1

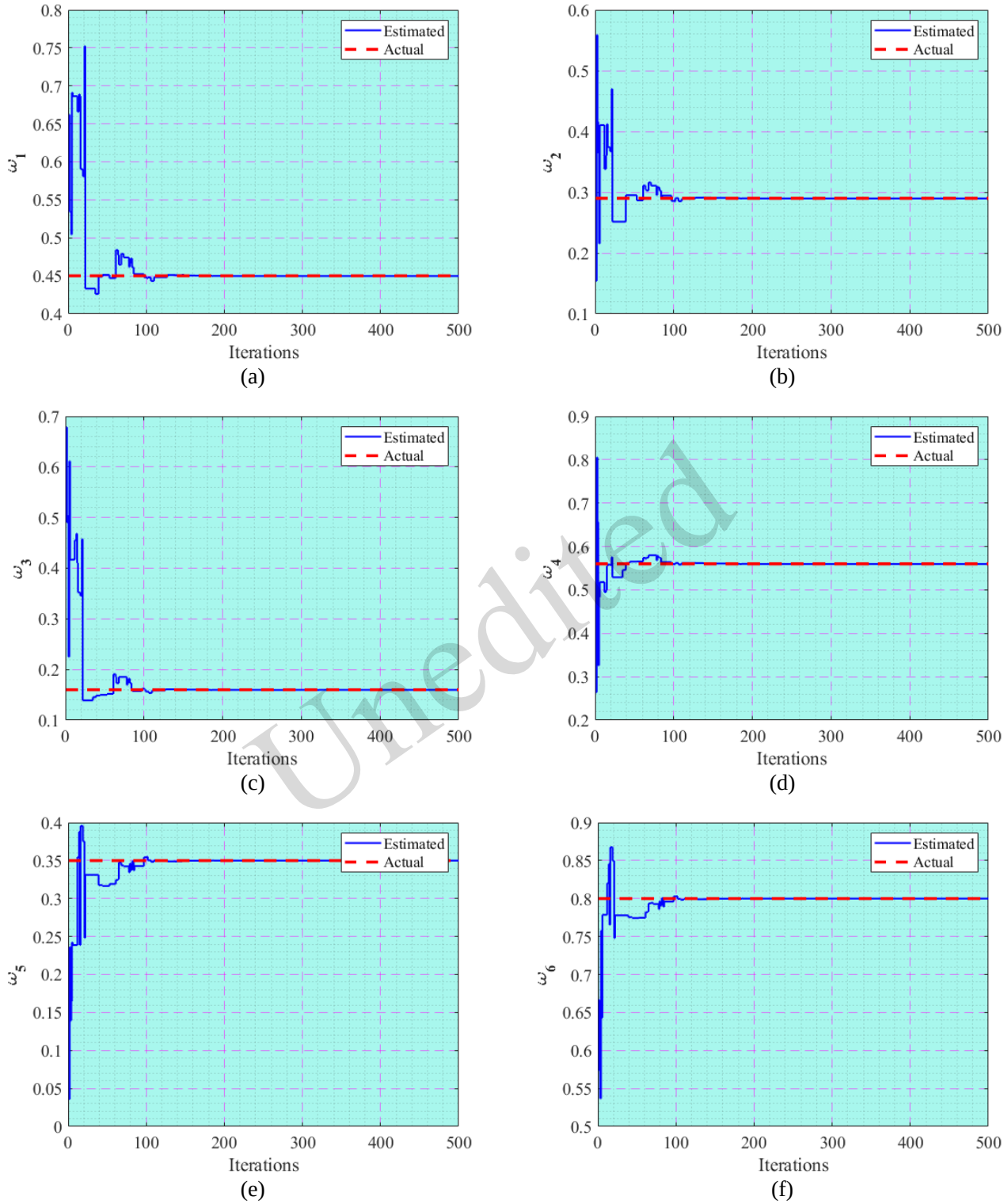

Fig. 7. Estimated parameters curves of the best independent run for $u = 0.00015$ in case study 1

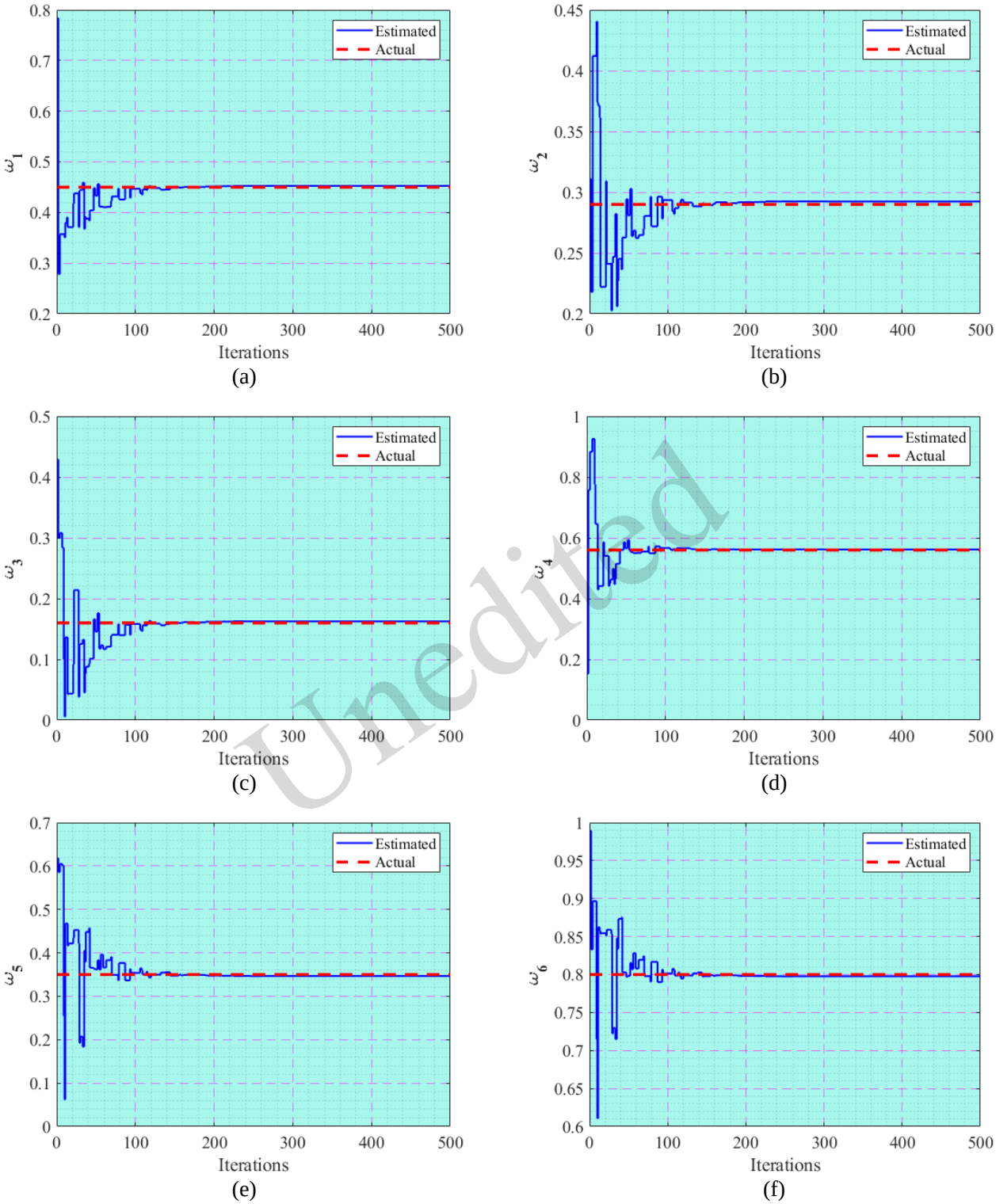

Fig. 8. Estimated parameters curves of the best independent run for $u = 0.0015$ in case study 1

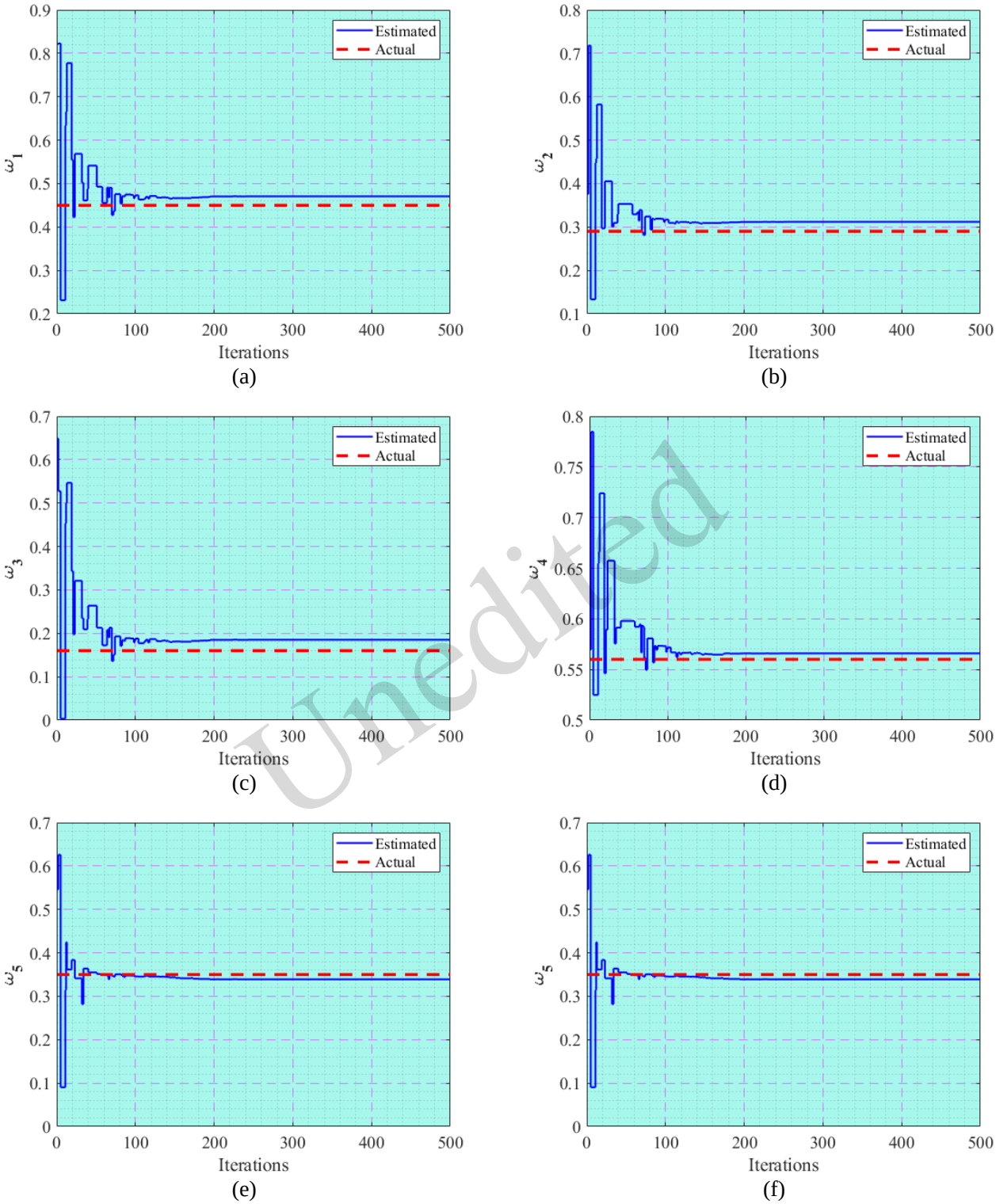

Fig. 9. Estimated parameters curves of the best independent run for $u = 0.015$ in case study 1

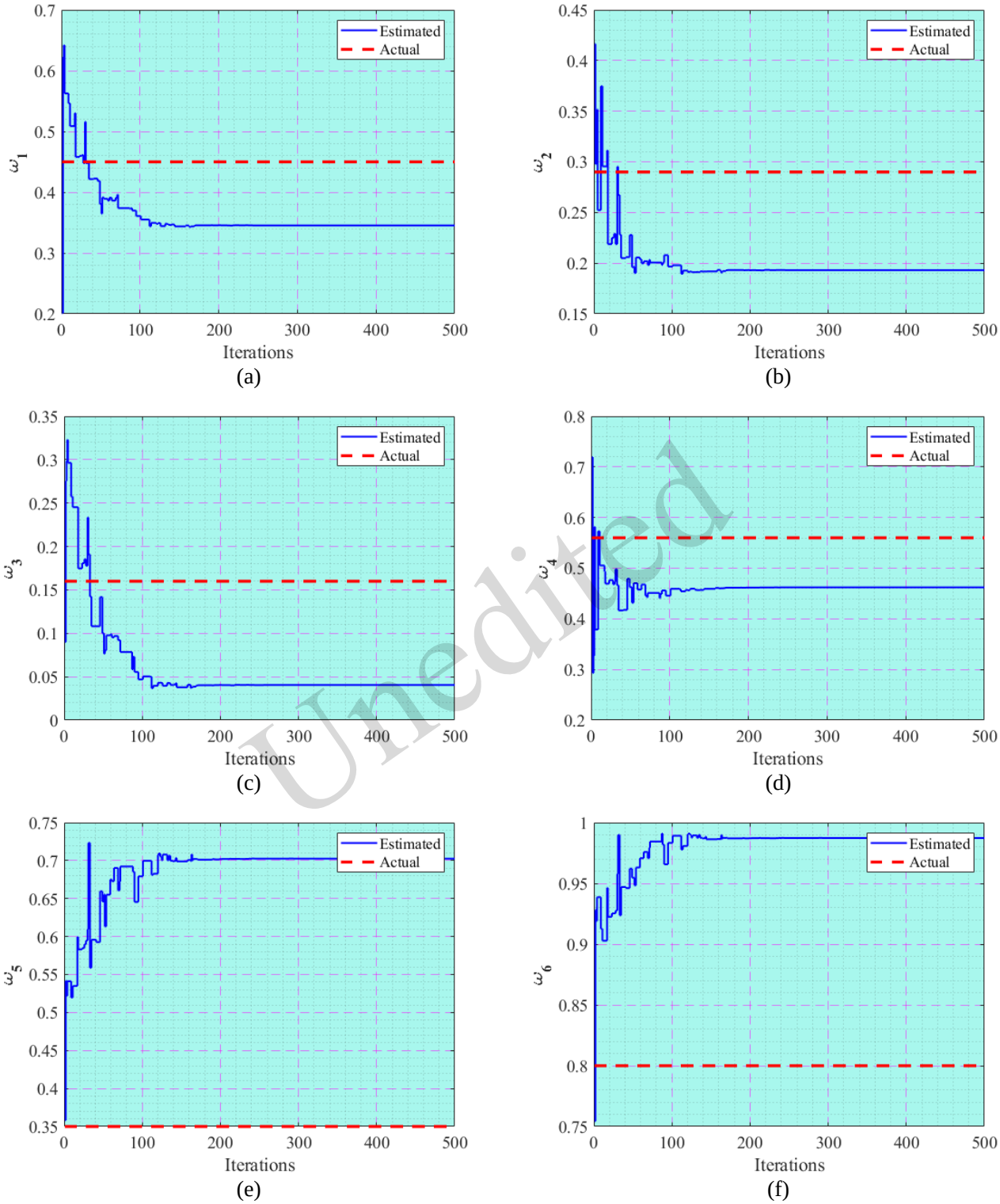

Fig. 10 Estimated parameters curves of the best independent run for $u = 0.15$ in case study 1

Table 1. Best estimated parameters for all noise scenarios of case study 1

Noise Levels	ω_1	ω_2	ω_3	ω_4	ω_5	ω_6
u = 0	0.4500	0.2900	0.1600	0.5600	0.3500	0.8000
u = 0.00015	0.4497	0.2897	0.1597	0.5597	0.3500	0.8000
u = 0.0015	0.4525	0.2924	0.1625	0.5617	0.3466	0.7977
u = 0.015	0.4707	0.3118	0.1853	0.5659	0.3390	0.7958
u = 0.15	0.3454	0.1931	0.0405	0.4621	0.7026	0.9874

Table 2. Comparison: Ranks of fitness, from best to worst, along with standard deviations for case study 1

Noise Levels	Best Fitness	Mean Fitness	Worst Fitness	Standard Deviation
u = 0	0.00000E+00	4.96017E-33	5.39569E-32	8.90802E-33
u = 0.00015	1.27892E-08	1.27892E-08	1.27894E-08	2.82445E-14
u = 0.0015	1.42604E-06	1.42606E-06	1.42668E-06	9.90498E-11
u = 0.015	1.63598E-04	1.63598E-04	1.63598E-04	2.76177E-12
u = 0.15	2.06484E-02	2.06484E-02	2.06485E-02	2.02044E-09

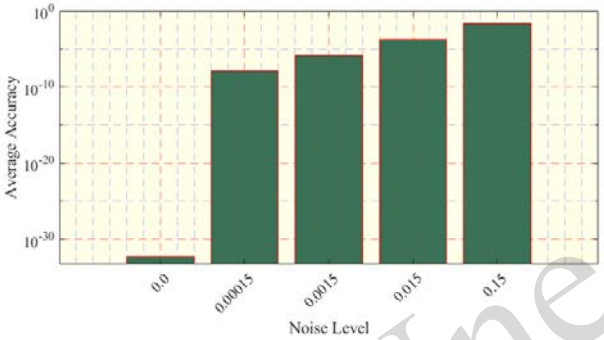

Fig. 11. Comparison of average accuracy for different noise scenarios in case study 1

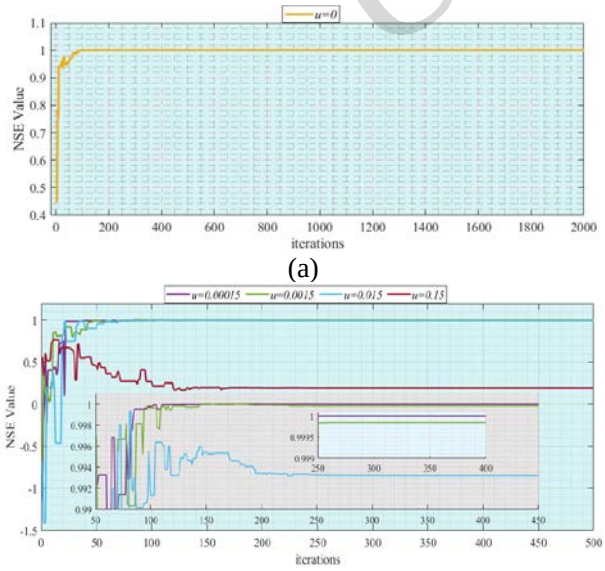

(a)

(b)

Fig. 12. NSE based curves for all disturbance levels of case study 1.

5 Conclusions

In this study, the identification problem of a fractional Hammerstein autoregressive with exogenous noise, HARX, is addressed using the swarm intelligent computing of the electric eel foraging optimization algorithm (EEFOA). The key term separation principle is incorporated to reduce the redundant parameters that occur due to cross-product terms in the system's information vector. The proposed scheme was evaluated for five different noise scenarios and various degrees of freedom in two different fractional-HARX models with variation in the order of nonlinearity. The efficiency, robustness, and accuracy of the system were validated through learning curve plots, statistical analyses, and weight estimation plots. However, the plots of the Nash–Sutcliffe efficiency metric advocate the performance and stability of the EEFOA for the fractional-HARX model. The statistical results in terms of best, average, and worst fitness values and standard deviation for five distinct noise scenarios confirm the efficacy of the EEFOA for the estimation of parameters in fractional-HARX models, even for stiff 3rd-order nonlinear fractional-HARX. The EEFOA and AVOA achieve a fitness value of level 10^{-6}, WOA and HOA obtain a fitness value of around 10^{-4}, and RSA provides a 10^{-3} fitness value for a 0.0015 noise scenario. Thus, the given methodology is verified to be accurate in comparison with recent counterpart optimization algorithms as endorsed by exhaustive simulations of various scenarios. In the future, applications of the proposed

computing approach can be explored in solving the battery state of charge estimation (Li Z et al., 2023b; Li Z et al., 2024) and hydropower generation problems (Wang P et al., 2023a; Wang P et al., 2023b; Zhao Z et al., 2022).

Contributors

Faisal ALTAF and Taimoor Ali KHAN drafted the manuscript. Muhammad Asif Zahoor RAJA and Naveed Ishtiaq CHAUDHARY designed the research. Ching-Lung CHANG supervised the research. Chi-Min SHU provided the resources and administered the project. Naveed Ishtiaq CHAUDHARY and Zeshan Aslam KHAN revised and finalized the paper

Compliance with ethics guidelines

All authors declare that they have no conflict of interest.

References

Abdollahzadeh B, Gharehchopogh FS, Mirjalili S, 2021. African vultures optimization algorithm: a new nature-inspired metaheuristic algorithm for global optimization problems. *Comput Ind Eng*, 158:107408. https://doi.org/10.1016/j.cie.2021.107408

Abdollahzadeh B, Khodadadi N, Barshandeh S, et al., 2024. Puma optimizer (PO): a novel metaheuristic optimization algorithm and its application in machine learning. *Cluster Comput*, 27(4):5235-5283. https://doi.org/10.1007/s10586-023-04221-5

Abualigah L, Abd Elaziz M, Sumari P, et al., 2022. Reptile search algorithm (RSA): a nature-inspired meta-heuristic optimizer. *Expert Syst Appl*, 191:116158. https://doi.org/10.1016/j.eswa.2021.116158

Ala A, Goli A, Mirjalili S, et al., 2024. A fuzzy multi-objective optimization model for sustainable healthcare supply chain network design. *Appl Soft Comput*, 150:111012. https://doi.org/10.1016/j.asoc.2023.111012

Ali R, Asjad MI, Akgül A, 2021. An analysis of a mathematical fractional model of hybrid viscous nanofluids and its application in heat and mass transfer. *J Comput Appl Math*, 383:113096. https://doi.org/10.1016/j.cam.2020.113096

Altaf F, Chang CL, Chaudhary NI, et al., 2024. Astrophysical expedition: transit search heuristics for fractional Hammerstein control autoregressive models. *Mod Phys Lett B*, in press, 2450417. https://doi.org/10.1142/S0217984924504177

Dong RY, Sun LX, Ma L, et al., 2023. Boosting Kernel search optimizer with slime mould foraging behavior for combined economic emission dispatch problems. *J Bionic Eng*, 20(6):2863-2895. https://doi.org/10.1007/s42235-023-00408-z

El-Hasnony IM, Barakat SI, Mostafa RR, 2020. Optimized ANFIS model using hybrid metaheuristic algorithms for Parkinson's disease prediction in IoT environment. *IEEE Access*, 8:119252-119270. https://doi.org/10.1109/ACCESS.2020.3005614

Fang LL, Liang XY, 2023. A novel method based on nonlinear binary grasshopper whale optimization algorithm for feature selection. *J Bionic Eng*, 20(1):237-252. https://doi.org/10.1007/s42235-022-00253-6

Frikh ML, Boutasseta N, 2024. Pitch angle control of wind turbines using model-free auto-tuned fractional order proportional derivative ATFOPD controller. *Comput Electr Eng*, 116:109199. https://doi.org/10.1016/j.compeleceng.2024.109199

Gamini S, Kumar SS, 2023. Homomorphic filtering for the image enhancement based on fractional-order derivative and genetic algorithm. *Comput Electr Eng*, 106:108566. https://doi.org/10.1016/j.compeleceng.2022.108566

González-Patiño D, Villuendas-Rey Y, Argüelles-Cruz AJ, et al., 2019. A novel bio-inspired method for early diagnosis of breast cancer through mammographic image analysis. *Appl Sci*, 9(21):4492. https://doi.org/10.3390/app9214492

Han Y, Chen WB, Heidari AA, et al., 2023. Multi-verse optimizer with rosenbrock and diffusion mechanisms for multilevel threshold image segmentation from COVID-19 chest X-ray images. *J Bionic Eng*, 20(3):1198-1262. https://doi.org/10.1007/s42235-022-00295-w

Heidari AA, Mirjalili S, Faris H, et al., 2019. Harris hawks optimization: algorithm and applications. *Future Gener Comput Syst*, 97:849-872. https://doi.org/10.1016/j.future.2019.02.028

Hu HY, Xie ZK, Wang DQ, 2024. Temporal pattern attention based Hammerstein model for estimating battery SOC. *J Energy Storage*, 100:113666. https://doi.org/10.1016/j.est.2024.113666

Ionescu C, Lopes A, Copot D, et al., 2017. The role of fractional calculus in modeling biological phenomena: a review. *Commun Nonlinear Sci Numer Simul*, 51:141-159. https://doi.org/10.1016/j.cnsns.2017.04.001

Jakšić Z, Devi S, Jakšić O, et al., 2023. A comprehensive review of bio-inspired optimization algorithms including applications in microelectronics and nanophotonics. *Biomimetics*, 8(3):278. https://doi.org/10.3390/biomimetics8030278

Karaca Y, 2023. Fractional calculus operators-Bloch torrey-partial differential equation-artificial neural networks-computational complexity modeling of the micro-macrostructural brain tissues with diffusion MRI signal processing and neuronal multi-components. *Fractals*, 31(10):2340204. https://doi.org/10.1142/S0218348X23402041

Kausar A, Chang CY, Raja MAZ, et al., 2025. A novel design of layered recurrent neural networks for fractional order Caputo–Fabrizio stiff electric circuit models. *Mod Phys Lett B*, 39(2):2450393. https://doi.org/10.1142/S0217984924503937

Khan TA, Chaudhary NI, Khan ZA, et al., 2024a. Design of Runge-Kutta optimization for fractional input nonlinear autoregressive exogenous system identification with key-term separation. *Chaos Solitons Fractals*, 182:114723. https://doi.org/10.1016/j.chaos.2024.114723

Khan TA, Chaudhary NI, Hsu CC, et al., 2024b. A gazelle optimization expedition for key term separated fractional nonlinear systems with application to electrically stimulated muscle modeling. *Chaos Solitons Fractals*, 185:115111. https://doi.org/10.1016/j.chaos.2024.115111

Li F, Zhu XJ, Cao QF, 2023a. Parameter learning for the nonlinear system described by a class of Hammerstein models. *Circuits Syst Signal Process*, 42(5):2635-2653. https://doi.org/10.1007/s00034-022-02240-y

Li F, Liang MJ, Luo YS, 2023b. Correlation analysis-based parameter learning of Hammerstein nonlinear systems with output noise. *Eur J Control*, 72:100819. https://doi.org/10.1016/j.ejcon.2023.100819

Li F, Zheng T, Cao QF, 2023c. Modeling and identification for practical nonlinear process using neural fuzzy network–based Hammerstein system. *Trans Inst Meas Control*, 45(11):2091-2102. https://doi.org/10.1177/01423312221143777

Li F, Zhou SB, Liu RR, 2024. Parameter estimation for the Hammerstein-Wiener nonlinear system and application in lithium-ion batteries. *J Energy Storage*, 102:114265. https://doi.org/10.1016/j.est.2024.114265

Li S, Huang CD, Song XS, 2023. Novel method to detect Hopf bifurcation in a delayed fractional-order network model with bidirectional ring structure. *Int J Biomath*, 16(6):2250117. https://doi.org/10.1142/S1793524522501170

Li ZQ, Wang WW, Zhang CL, et al., 2023. Fault-tolerant control based on fractional sliding mode: crawler plant protection robot. *Comput Electr Eng*, 105:108527. https://doi.org/10.1016/j.compeleceng.2022.108527

Li ZX, Yang Y, Li LW, et al., 2023. A weighted Pearson correlation coefficient based multi-fault comprehensive diagnosis for battery circuits. *J Energy Storage*, 60:106584. https://doi.org/10.1016/j.est.2022.106584

Li ZX, Li LW, Chen J, et al., 2024. A multi-head attention mechanism aided hybrid network for identifying batteries' state of charge. *Energy*, 286:129504. https://doi.org/10.1016/j.energy.2023.129504

Liu X, Wang C, Dai W, 2024. Probability-based identification of Hammerstein systems with asymmetric noise characteristics. *IEEE Trans Instrum Meas*, 73:6500611. https://doi.org/10.1109/TIM.2023.3336437

Machado JAT, Lopes AM, 2015. Analysis of natural and artificial phenomena using signal processing and fractional calculus. *Fract Calc Appl Anal*, 18(2):459-478. https://doi.org/10.1515/fca-2015-0029

Malik MF, Chang CL, Aslam MS, et al., 2022. Fuzzy-evolution computing paradigm for fractional Hammerstein control autoregressive systems. *Int J Fuzzy Syst*, 24(5):2447-2475. https://doi.org/10.1007/s40815-022-01291-2

Malik MF, Chang CL, Chaudhary NI, et al., 2023. Swarming intelligence heuristics for fractional nonlinear autoregressive exogenous noise systems. *Chaos Solitons Fractals*, 167:113085. https://doi.org/10.1016/j.chaos.2022.113085

Malik NA, Chang CL, Chaudhary NI, et al., 2024. Astrophysics-based transit search optimization heuristics for parameter estimation of multi-frequency sinusoidal signals. *Mod Phys Lett B*, 38(34):2450342. https://doi.org/10.1142/S0217984924503421

Mathi MT, Baburaj E, 2022. Comparative analysis of bio-inspired optimization algorithms in neural network-based data mining classification. *Int J Swarm Intell Res*, 13(1):25. https://doi.org/10.4018/IJSIR.2022010103

Megherbi O, Hamiche H, Bettayeb M, 2024. Implementation of a wireless text data transmission based on the impulsive control of fractional-order chaotic systems. *Comput Electr Eng*, 116:109224. https://doi.org/10.1016/j.compeleceng.2024.109224

Mehmood K, Chaudhary NI, Khan ZA, et al., 2024. Atomic physics-inspired atom search optimization heuristics integrated with chaotic maps for identification of electro-hydraulic actuator systems. *Mod Phys Lett B*, 38(30):2450308. https://doi.org/10.1142/S0217984924503081

Mehmood N, Abbas A, Akgül A, et al., 2023. Existence and stability results for coupled system of fractional differential equations involving AB-Caputo derivative. *Fractals*, 31(2):2340023. https://doi.org/10.1142/S0218348X23400236

Mirjalili S, Lewis A, 2016. The whale optimization algorithm. *Adv Eng Softw*, 95:51-67. https://doi.org/10.1016/j.advengsoft.2016.01.008

Mukhtar R, Chang CY, Raja MAZ, et al., 2024. Novel nonlinear fractional order Parkinson's disease model for brain electrical activity rhythms: intelligent adaptive Bayesian networks. *Chaos Solitons Fractals*, 180:114557. https://doi.org/10.1016/j.chaos.2024.114557

Padhi JR, Deeb MA, Tripathy S, et al., 2023. Fractional calculus based PI-FOPID controller for frequency deviation control in integrated power system. Control Applications in Modern Power Systems: Select Proceedings of EPREC 2022, p.213-224. Singapore: Springer.

Partohaghighi M, Yusuf A, Alshomrani AS, et al., 2024. Fractional hyper-chaotic system with complex dynamics and high sensitivity: applications in engineering. *Int J Mod Phys B*, 38(1):2450012. https://doi.org/10.1142/S0217979224500127

Rahmanshahi M, Jafari-Asl J, Fathi-Moghadam M, et al., 2024. Metaheuristic learning algorithms for accurate prediction of hydraulic performance of porous embankment weirs. *Appl Soft Comput*, 151:111150. https://doi.org/10.1016/j.asoc.2023.111150

Šapina M, Garcin M, Kramarić K, et al., 2020. The Hurst exponent of heart rate variability in neonatal stress, based on a mean-reverting fractional Lévy stable motion. *Fluctuation Noise Lett*, 19(3):2050026. https://doi.org/10.1142/S0219477520500261

Sowa M, Majka Ł, Wajda K, 2023. Excitation system voltage regulator modeling with the use of fractional calculus. *AEU-Int J Electron Commun*, 159:154471. https://doi.org/10.1016/j.aeue.2022.154471

Sweis H, Arqub OA, Shawagfeh N, 2023. Fractional delay integrodifferential equations of nonsingular kernels: existence, uniqueness, and numerical solutions using Galerkin algorithm based on shifted Legendre polynomials. *Int J Mod Phys C*, 34(4):2350052. https://doi.org/10.1142/S0129183123500523

Tubishat M, Al-Obeidat F, Sadiq AS, et al., 2023. An improved dandelion optimizer algorithm for spam detection: next-generation email filtering system. *Computers*, 12(10):196. https://doi.org/10.3390/computers12100196

Vyawahare VA, Nataraj PSV, 2013. Fractional-order modeling of neutron transport in a nuclear reactor. *Appl Math Modell*, 37(23):9747-9767. https://doi.org/10.1016/j.apm.2013.05.023

Wang DQ, 2024. Key-term separation based hierarchical gradient approach for NN based Hammerstein battery model. *Appl Math Lett*, 157:109207. https://doi.org/10.1016/j.aml.2024.109207

Wang PF, Guo YX, Xu ZK, et al., 2023a. A novel approach of full state tendency measurement for complex systems based on information causality and PageRank: a case study of a hydropower generation system. *Mech Syst Signal Process*, 187:109956. https://doi.org/10.1016/j.ymssp.2022.109956

Wang PF, Xu ZK, Chen DY, 2023b. An integrated framework for reliability prediction and condition-based maintenance policy for a hydropower generation unit using GPHM and SMDP. *Reliab Eng Syst Saf*, 238:109419. https://doi.org/10.1016/j.ress.2023.109419

Wang SW, Xiao XP, Ding Q, 2024. A novel fractional system grey prediction model with dynamic delay effect for evaluating the state of health of lithium battery. *Energy*, 290:130057. https://doi.org/10.1016/j.energy.2023.130057

Ye SQ, Zhou KQ, Zain AM, et al., 2023. A modified harmony search algorithm and its applications in weighted fuzzy production rule extraction. *Front Inform Technol Electron Eng*, 24(11):1574-1590. https://doi.org/10.1631/FITEE.2200334

Zhang MG, Li F, Yu Y, et al., 2024. Estimation of Hammerstein nonlinear systems with noises using filtering and recursive approaches for industrial control. *Front Inform Technol Electron Eng*, 25(2):260-271. https://doi.org/10.1631/FITEE.2300620

Zhang XF, Boutat D, Liu DY, 2023. Applications of fractional operator in image processing and stability of control systems. *Fractal Fract*, 7(5):359. https://doi.org/10.3390/fractalfract7050359

Zhao WG, Wang LY, Zhang ZX, et al., 2024. Electric eel foraging optimization: a new bio-inspired optimizer for engineering applications. *Expert Syst Appl*, 238:122200. https://doi.org/10.1016/j.eswa.2023.122200

Zhao ZW, Yuan YC, He MJ, et al., 2022. Stability and efficiency performance of pumped hydro energy storage system for higher flexibility. *Renew Energy*, 199:1482-1494. https://doi.org/10.1016/j.renene.2022.09.085

Appendix: FITEE_ESM

Appendix. The results for case study 2 of a fractional-HARX system with 3rd-order nonlinearity are provided in the Supplementary Material.